Journal of Materials Chemistry B

RSC Publishing

PAPER

View Article Online
View Journal | View Issue

Cite this: *J. Mater. Chem. B*, 2013, **1**, 361

A graphene oxide platform for the assay of DNA 3′-phosphatases and their inhibitors based on hairpin primer and polymerase elongation†

Wenping Zhu, Ziwei Zhao, Zhen Li, Jianhui Jiang,* Guoli Shen and Ruqin Yu*

Received 13th September 2012
Accepted 30th October 2012

DOI: 10.1039/c2tb00109h

www.rsc.org/MaterialsB

We have developed a label-free, simple and highly sensitive hairpin fluorescent biosensor for the assay of DNA 3′-phosphatases and their inhibitors utilizing a graphene oxide (GO) platform. In this assay, we designed a hairpin primer (HP) with a 3′-phosphoryl end that served as the substrate for DNA 3′-phosphatases. Once the phosphorylated HP was hydrolyzed by DNA 3′-phosphatases, the resulting HP with a 3′-hydroxyl end was immediately elongated to form a long double-strand product by Klenow fragment polymerase (KF polymerase). With SYBR green I (SG) selective staining of the double-helix DNA, a very high fluorescence enhancement was achieved. Furthermore, GO was introduced to quench the fluorescence of the HP without polymerase elongation, thereby further increasing the signal-to-background ratio. The proposed method is simple and convenient, yet still exhibits high sensitivity and selectivity. This method has been successfully applied to detecting the activity of two typical 3′-phosphatases, T4 polynucleotide kinase phosphatase (PNKP) and shrimp alkaline phosphatase (SAP). The effect of their inhibitors has also been investigated. The results revealed that the method allowed a sensitive quantitative assay of T4 PNKP and SAP, with detection limits of 0.07 U mL^{-1} and 0.003 U mL^{-1}, respectively. The proposed method is anticipated to find applications in the study of DNA damage repair mechanisms.

Introduction

DNA strand breaks bearing abnormal termini, known as blocking lesions, such as DNA terminated with a 3′-phosphate, result from exposure to both external genotoxic agents and endogenous sources of stress, and can be mutagenic and detrimental to survival.[1,2] Since these blocking lesions prevent the polymerization and ligation events necessary to re-establish the continuity of a DNA strand, removal of the abnormal termini is a prerequisite for DNA damage repair. DNA 3′-phosphatases play important roles in the repair of strand breaks induced by DNA damaging agents. All 3′-phosphate termini can be restored to hydroxyl groups by DNA 3′-phosphatases, by virtue of their 3′-phosphodiesterase activity.[3,4] In addition, many enzymes have been demonstrated to possess such a capacity, exemplified by the T4 polynucleotide kinase phosphatase (PNKP) and alkaline phosphatase. T4 PNKP is a bifunctional enzyme with 5′-kinase and 3′-phosphatase activities provided by two non-overlapping catalytic domains.[5] Alkaline phosphatases, such as shrimp alkaline phosphatase (SAP), show relatively lower activity and specificity in comparison with the PNKP enzymes. Considering their roles in the repair of strand breaks, sensitive and selective detection of DNA 3′-phosphatases is of great importance. To detect DNA 3′-phosphatases, several traditional methods such as absorption spectrophotometry,[6] immunoassays,[7] radical isotope ^{32}P-labelling, [5] polyacrylamide gel electrophoresis (PAGE),[2] and autoradiography[8] are commonly used. All these methods, however, are laborious and time-consuming, require specific instruments, show insufficient specificity and sensitivity, or necessitate radio-labelling. Recent efforts have been made towards the development of fluorescence assays for DNA 3′-phosphatases, but they all involve the use of costly fluorophore-labelled probes.[9,10] Therefore, the development of new analytical techniques for sensitive, selective, cost-effective and facile detection of DNA 3′-phosphatases is of considerable interest.

The label-free detection strategy has gained much interest because it can provide a fast and cost-effective assay. The use of intercalating dyes such as SYBR Green I (SG) is a common label-free detection method which has been developed as a fluorescent probe for the detection of nucleic acids,[11] protein[12] and metal ions.[13] However, like other intercalating dyes, SG still has a high background signal because of the non-specific

State Key Laboratory for Chemo/Biosensing and Chemometrics, College of Chemistry and Chemical Engineering, Hunan University, Changsha, 410082, P. R. China. E-mail: jianhuijiang@hnu.edu.cn; rqyu@hnu.edu.cn; Fax: +86-731-8822782; Tel: +86-731-8822577

† Electronic supplementary information (ESI) available: TEM image of GO, experiment optimization, selectivity and biological sample investigation. See DOI: 10.1039/c2tb00109h

adsorption of the dye to non-target nucleic acids and proteins. Hence, the reduction of the background signal of SG became a challenge in developing the new methodology.

Graphene is the newest member of the carbon materials family. Due to their excellent optical and electronic properties as well as excellent biocompatibility, graphene and its derivatives have attracted wide research interest in nanoelectronics,[14] biosensors[15] and nanocomposites.[16] To improve its solubility in water, graphene is oxidized to graphene oxide (GO) by generating surface carboxylic acid and hydroxyl groups. Recently, GO has been demonstrated to hold great potential in making DNA-based optical sensors for the detection of nucleic acids,[17,18] proteins,[19,20] metal ions,[21] and small molecules,[22,23] and for drug delivery.[24] Most GO-based DNA optical sensors rely on the preferential binding of GO to single-stranded DNA (ssDNA) over double-stranded DNA (dsDNA), thereby quenching the fluorescence of dyes conjugated to ssDNA. Previous reports demonstrated that GO could act as an efficient signal-to-background enhancer for DNA detection.[25]

Here we report a novel strategy for the assay of DNA 3′-phosphatases and their inhibitors by means of the efficient quenching ability of GO and cost-effective label-free detection. As far as we know, this is the first time that DNA 3′-phosphatase has been detected based on GO coupled with DNA intercalating dyes. The proposed method is simple, economical and convenient, and is also more sensitive and selective than most previous fluorophore-based GO platforms. In addition, the proposed method was able to quantitatively investigate the inhibition effect of inhibitors on DNA 3′-phosphatase. In contrast to previous GO-based DNA optical sensors using fluorophore-labelled DNA probes, the protocol utilized a label-free DNA hairpin primer (HP) acting as the substrate for DNA 3′-phosphatase. Once the 3′-phosphoryl end of the HP was hydrolyzed to a hydroxyl group, the polymerase elongation was initiated in the presence of Klenow fragment polymerase (KF polymerase) and deoxyribonucleoside triphosphates (dNTPs). The elongation reaction product with long dsDNA showed a great fluorescence enhancement upon staining with SG. After the addition of GO, the high background signal of HP without polymerase elongation was greatly quenched, whereas significant fluorescence quenching did not occur to the polymerase elongation products. The concentration of DNA 3′-phosphatase was directly proportional to the fluorescence intensity generated. By monitoring the fluorescence intensity change of the sensing system, the quantification of DNA 3′-phosphatase could be realized.

Experimental

Chemicals and materials

Bovine serum albumin (BSA), human immunoglobulin G (human IgG), platelet-derived growth factor (PDGF)-BB, streptavidin (SA) and SYBR Green I (10 000× concentrate) were obtained from Dingguo Biochemical Reagents (Beijing, China). T4 polynucleotide kinase phosphatase (PNKP), Klenow fragment polymerase (KF polymerase, without 3′ to 5′ exonuclease activity), and deoxyribonucleoside triphosphates (dNTPs) were purchased from New England Biolabs Ltd., Beijing, China. Shrimp alkaline phosphatase (SAP) was purchased from Fermentas Inc., MBI, Canada. Heparin, fetal bovine serum (FBS) and sodium orthovanadate (Na_3VO_4) were obtained from Sangon Biotechnology Co. Ltd., Shanghai, China. The DNA oligonucleotide used in this work was synthesized by Sangon Biotechnology Co. Ltd., Shanghai, China. The sequence of the DNA oligonucleotide is as follows, where the loop sequence is indicated in italics, and complementary sequences are underlined.

HP: 5′-TAGAGAGAGAGAGAGAGAGAGAGCGCACC*TAAAG* GGTGCG-phos-3′.

The buffer solutions employed in this work were the following: the reaction buffer was 10 mM Tris–HCl, 10 mM $MgCl_2$, 50 mM NaCl, and 1 mM DTT (pH 7.9); the detection buffer was 10 mM Tris–HCl, 100 mM NaCl, and 5 mM $MgCl_2$ (pH 8.0). GO was synthesized by a modified Hummers' method[26] (for characterization see Fig. S1, ESI†). All other reagents were of analytical grade and used without further purification. Deionized and sterilized water (resistance > 18.2 MΩ cm) was used throughout.

Apparatus

All fluorescence measurements were performed on a Hitachi F-7000 fluorescence spectrometer (Hitachi Ltd., Japan). The optical path length of a quartz fluorescence cell was 1.0 cm. Excitation and emission slits were all set for a 5.0 nm band-pass and 800 V was chosen as the excitation voltage. All fluorescence detections were carried out at room temperature unless otherwise indicated. Raman spectra were collected on a Jobin Yvon Micro-Raman spectrometer (RamLab-010, France). High Resolution Transmission Electron Microscopy (HRTEM) images were recorded using a JEM-3010 (Jeol).

Assay procedures

In a typical experiment, 2 μL aliquots of sample solution containing varying concentrations of T4 PNKP were added to a reaction mixture (23 μL) of HP (40 nM), KF polymerase (100 U mL^{-1}), dNTPs (50 μM) and incubated at 37 °C for 80 min. Then, 1 μL SG (100×) was added and the solution was kept at room temperature for 10 min. Finally, 3 μL GO (100 μg mL^{-1}) and the detection buffer were added to give a final volume of 100 μL. After 10 min, the fluorescence was measured and recorded on a Hitachi F-7000 fluorescence spectrometer. The assay procedure for SAP was slightly different. Firstly, varying concentrations of SAP were added to a reaction mixture (10 μL) containing 250 nM HP, and kept at 37 °C for 60 min. Then, the above solution was heated at 65 °C for 15 min to inactivate SAP. KF polymerase, dNTPs and the reaction buffer were added to give a final reaction volume of 25 μL, and then the reaction solution was incubated at 37 °C for 60 min. The following experimental steps with the addition of SG and GO were the same as for T4 PNKP, except that 8 μL GO (100 μg mL^{-1}) was added instead of 3 μL GO. Fluorescence detection was performed at room temperature, and the excitation and emission wavelengths were set to 497 and 524 nm, respectively.

Inhibition of the dephosphorylation reaction

The two inhibitors used here were heparin and Na_3VO_4. The effect of heparin on the 3′-phosphatase activity of T4 PNKP was investigated according to the following procedure: T4 PNKP (100 U mL^{-1}) was firstly mixed with varying concentrations of heparin, then HP, KF polymerase, dNTPs and reaction buffer were added to give a final reaction volume of 25 μL, and the above solution was kept at 37 °C for 80 min. The following experimental steps with the addition of SG and GO were the same as those for the assay of T4 PNKP. The effect of Na_3VO_4 on the 3′-phosphatase activity of SAP was tested according to a similar procedure: SAP (2 U mL^{-1}) mixed with varying concentrations of Na_3VO_4 was added to a reaction mixture (10 μL) containing 250 nM HP, then the mixture was kept at 37 °C for 60 min. The following steps of inactivation, polymerase elongation and the addition of SG and GO were the same as the above assay procedure for SAP.

Gel electrophoresis analysis

Electrophoresis analysis was carried out on 4% agarose gels by GoldView staining, casting and running in 0.5 × TBE buffer (45 mM Tris, 45 mM boric acid, 1.25 mM EDTA, pH 7.9) at room temperature. The electrophoresis procedure was performed at a constant potential of 110 V for 90 min with a loading of 10 μL of each sample into the lanes. The resulting gel was excited using a WD-9403F UV device and imaged with a Canon digital camera.

Results and discussion

The proposed strategy for the label-free assay of DNA 3′-phosphatases and their inhibitors relies on the fact that the staining of double-strand polymerase elongation product with SG could result in high fluorescence enhancement and the preferential binding of GO with ssDNA over dsDNA. The principal design of our approach is illustrated in Scheme 1. The DNA primer contains two short single stranded self-complementary sequences which can form a hairpin structure with a 3′-phosphoryl end under appropriate hybridizing conditions. Because the polymerase elongation reaction is only initiated at the 3′-hydroxyl end of the primer, the 3′-phosphorylated HP formed in such a way is an inactive substrate for KF polymerase in the absence of T4 PNKP or SAP, and thus cannot trigger the polymerase elongation. When stained with SG followed by the addition of GO, the fluorescence is greatly quenched, giving a weak background for the sensing system. However, the HP can be dephosphorylated into a 3′-hydroxyl end by DNA 3′-phosphatase, which then can serve as the preferred substrate for KF polymerase. Therefore, in the presence of T4 PNKP or SAP, together with the KF polymerase and dNTPs, polymerase elongation is initiated to generate a long double-helix hairpin product. With SG selective staining of the elongation product, a significant fluorescence emission is generated. Because of the weak affinity between the double-helix DNA and GO, significant fluorescence quenching will not occur for the elongation product, leading to a strong fluorescence signal after the addition of GO. Combining the unique properties of GO and SG, a label-free sensitive fluorescent sensing system with a high signal-to-background ratio has been constructed.

To verify that the increase of fluorescence signal was indeed caused by the binding of SG with the polymerase elongation product and the polymerase elongation was initiated by dephosphorylating HP using DNA 3′-phosphatase, a proof of principle experiment was carried out in the absence of T4 PNKP and SAP or in the presence of inactivated T4 PNKP and SAP.

As shown in Fig. 1A, in the absence of T4 PNKP or SAP, the polymerase elongation is not induced and as a result rather weak fluorescence signals were obtained (curves a_0 and b_0). Two similarly weak fluorescence signals were also observed in the presence of inactivated T4 PNKP or SAP (curves a_0' and b_0').

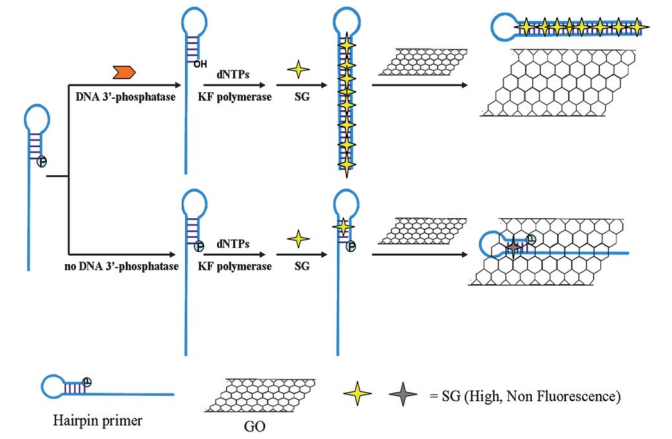

Scheme 1 Schematic illustrating the principle mechanism involved in the label-free fluorescent assay for DNA 3′-phosphatases and their inhibitors.

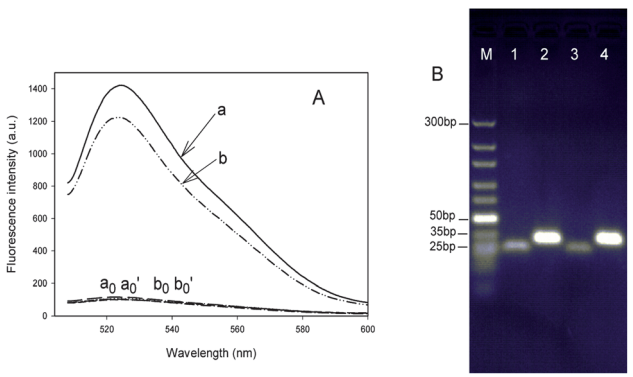

Fig. 1 (A) The fluorescence emission spectra under different conditions: (a) 100 U mL^{-1} T4 PNKP, 40 nM HP, 100 U mL^{-1} KF polymerase and 50 μM dNTPs; (a_0) 40 nM HP, 100 U mL^{-1} KF polymerase and 50 μM dNTPs; (a_0') 100 U mL^{-1} inactivated T4 PNKP, 40 nM HP, 100 U mL^{-1} KF polymerase and 50 μM dNTPs; (b) 2 U mL^{-1} SAP, 100 nM HP, 200 U mL^{-1} KF polymerase and 100 μM dNTPs; (b_0) 100 nM HP, 200 U mL^{-1} KF polymerase and 100 μM dNTPs; (b_0') 2 U mL^{-1} inactivated SAP and 100 nM HP, 200 U mL^{-1} KF polymerase and 100 μM dNTPs. (B) Gel electrophoresis images for the label-free assay of DNA 3′-phosphatases before and after polymerase elongation. Lane M: DNA size marker (10–300 bp); lane 1: HP without T4 PNKP; lane 2: HP with T4 PNKP; lane 3: HP without SAP; lane 4: HP with SAP.

These fluorescence background signals originated from the SG stained HP, which showed a relatively weak affinity for GO compared with ssDNA. In the presence of T4 PNKP (100 U mL^{-1}) or SAP (2 U mL^{-1}), two much stronger fluorescence signals were observed with a signal-to-background ratio of more than 10 (curves a and b), implying the formation of the long double-helix elongation product. These experimental results demonstrated the feasibility of the proposed strategy for the detection of DNA 3′-phosphatase.

To further verify the feasibility of the proposed strategy, an electrophoresis experiment was performed. Fig. 1B displays the typical gel electrophoresis images observed in the absence and presence of T4 PNKP or SAP. As shown in Fig. 1B, in the absence of T4 PNKP or SAP, the polymerase elongation could not be initiated for HP in lanes 1 and 3, thereby a weak DNA band was observed in lanes 1 and 3. Whereas, in the presence of T4 PNKP or SAP, the HP in lanes 2 or 4 was dephosphorylated and underwent polymerase elongation, resulting in a significant bright band in lanes 2 and 4, respectively. Additionally, the DNA bands in lanes 2 and 4 exhibited relatively low mobility in comparison with the DNA bands in lanes 1 and 3, demonstrating the impressive increase in the amount of double-helix DNA, the elongation products. The electrophoresis results provided further evidence for the feasibility of the proposed strategy.

Study of GO as a signal-to-background enhancer

Additional experiments were performed to study the use of GO as a signal-to-background enhancer. Experiments were performed with the addition of GO and compared to the results with no GO usage.

As shown in Fig. 2, the signal-to-background ratio (F_c/F_d) without the addition of GO was 3.23, while the ratio ($F_{c'}/F_{d'}$) increased to 16.77 after 8 μg mL^{-1} GO was added, confirming that GO acts as an efficient signal-to-background enhancer. The signal-to-background (S/N) ratio without addition of GO (under the optimal experimental conditions) and its comparison with that with the addition of GO are displayed in Fig. S6 (ESI†).

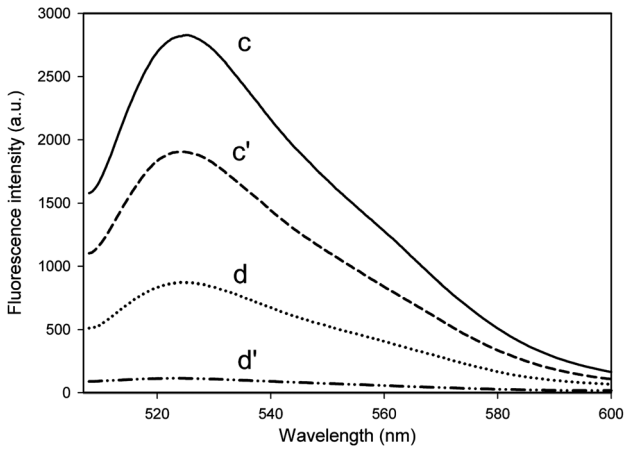

Fig. 2 The fluorescence emission spectra under different conditions: (c) 100 nM HP with 100 U mL^{-1} T4 PNKP; (d) 100 nM HP without T4 PNKP; (c′) 100 nM HP with 100 U mL^{-1} T4 PNKP after the addition of 8 μL GO (100 μg mL^{-1}); (d′) 100 nM HP without T4 PNKP after the addition of 8 μL GO (100 μg mL^{-1}). F_c, $F_{c'}$, F_d, and $F_{d'}$ are the fluorescence peak responses at 524 nm of curves c, c′, d and d′, respectively.

Optimization of assay conditions

The concentration of HP is a crucial parameter for the dephosphorylation process and the polymerase elongation. In order to optimize the HP concentration, we firstly investigated the optimal amount of GO for each HP concentration (data not shown). Then, the concentration of DNA 3′-phosphatase was kept constant and we compared the signal-to-background ratio of varying concentrations of HP with their optimal GO usage. Taking lower detection limits into consideration, the concentrations of T4 PNKP and SAP were kept at 4 U mL^{-1} and 0.1 U mL^{-1}, respectively. Fig. S2 and S3 (ESI†) depict the optimization results of the HP concentration for assaying T4 PNKP and SAP, respectively. As shown in Fig. S2,† F_1/F_{blank1} reached a maximum at 40 nM of HP, and decreased gradually along with the HP concentration up to 140 nM. Thus, the optimal concentration of HP for assaying T4 PNKP was chosen to be 40 nM, and was used throughout subsequent experiments. The optimized results for SAP detection are shown in Fig. S3.† It was noticed that F_2/F_{blank2} increased with the increase of HP concentration at first then decreased after 100 nM of HP, displaying a peak-shape dependency on the HP concentration with a maximum achieved using 100 nM HP. Therefore, the optimal concentration of HP for assaying SAP was 100 nM, and was used throughout subsequent experiments. Moreover, to achieve the best sensing performance, the reaction time and the concentrations of KF polymerase and dNTPs were also optimized (see ESI, Fig. S4 and S5†); experimental results showed that the following conditions provided the maximum S/N ratio for the sensing system: 40 nM HP, 100 U mL^{-1} KF polymerase, 50 μM dNTPs and a reaction time of 80 min for T4 PNKP; 100 nM HP, 200 U mL^{-1} KF polymerase, 100 μM dNTPs and an incubation time of 60 min for the dephosphorylation process of SAP.

Application of the GO platform for T4 PNKP detection

We chose the fluorescence emission from SG at 524 nm to evaluate the performances of the proposed method. The activity of T4 PNKP was quantified based on the optimal experimental conditions.

Fig. 3A depicts the typical fluorescence spectral responses of the hairpin fluorescent biosensor to T4 PNKP at varying concentrations. One can observe dynamically increased fluorescence peaks with increasing T4 PNKP concentration ranging from 0.1 to 400 U mL^{-1}. The peak intensity showed a linear correlation to T4 PNKP concentration in the range of 0.2 to 100 U mL^{-1}, as shown in Fig. 3B. The linear relationship can be described as $F = 155.9 + 12.88C$ (F is the fluorescence intensity and C is the concentration of T4 PNKP), and the correlation coefficient $R^2 = 0.995$. The detection limit was estimated to be 0.07 U mL^{-1} according to the 3σ rule, which was much lower than the previously reported fluorescent assay based on a universal molecular beacon and quantitative real-time PCR,[9]

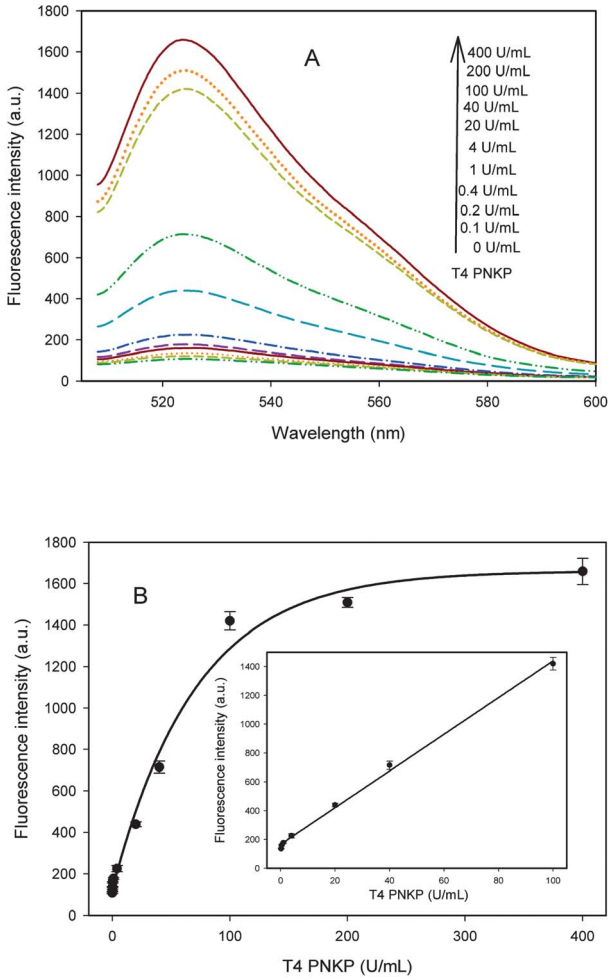

Fig. 3 (A) Typical fluorescence spectral responses of the label-free hairpin fluorescent biosensor to T4 PNKP at varying concentrations. (B) Fluorescence response at 524 nm of the label-free DNA 3′-phosphatase assay *versus* T4 PNKP concentration. Error bars are standard deviation (SD) across three repeated experiments. Experimental conditions were the optimized conditions shown in the Experimental section.

and comparable to another fluorescent assay based on a coupled exonuclease reaction and a graphene oxide platform.[27] The results demonstrated that the proposed method could be used as a highly sensitive fluorescent biosensor for T4 PNKP detection.

Because of the homogeneous assay format, the proposed method also showed good reproducibility. A series of four repeated assays were performed for detecting 100 U mL^{-1} and 20 U mL^{-1} of T4 PNKP, and the relative standard deviations (RSDs) were 4.2% and 4.5%, respectively. The results indicated that the proposed method had an acceptable reproducibility and precision.

The proposed method also exhibited high selectivity toward T4 PNKP over other interfering species. Fig. S7† depicts the selectivity of the sensing platform for T4 PNKP detection compared to other interfering proteins. As shown in Fig. S7,† the fluorescent sensor yielded very weak fluorescence responses to other proteins such as BSA, IgG, PDGF-BB and SA, which contrasted clearly with the strong fluorescence response to T4 PNKP. The results obviously indicated that the proposed method had superior selectivity towards T4 PNKP and was able to detect T4 PNKP among other interfering proteins.

Application of the GO platform for SAP detection

To demonstrate the generality of this design, the proposed method was also designed for SAP detection. Fig. 4A depicts the typical fluorescence spectral responses of the hairpin fluorescent biosensor to SAP at varying concentrations. It is observed that the fluorescence signals gradually increased as the concentration of SAP varied from 0.004 to 10 U mL^{-1}. The dependence of the fluorescence signal on SAP concentration is displayed in Fig. 4B. The fluorescence signal increased linearly with the SAP concentration in the range from 0.004 to 0.4 U mL^{-1}. The linear calibration equation was $F = 911.2C + 121.6$, with the correlation coefficient $R^2 = 0.999$, where F is the fluorescence intensity and C is the concentration of SAP. The detection limit of SAP was 0.003 U mL^{-1} according to the 3σ rule, which was two orders of magnitude lower than a previously

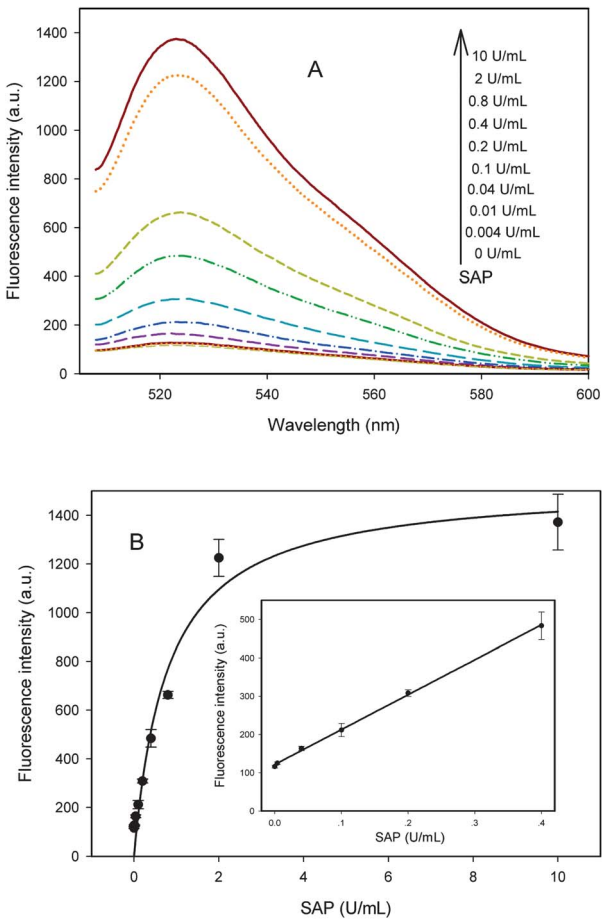

Fig. 4 (A) Typical fluorescence spectral responses of the label-free hairpin fluorescent biosensor to SAP at varying concentrations. (B) Fluorescence response at 524 nm of the label-free DNA 3′-phosphatase assay *versus* SAP concentration. Error bars are standard deviation (SD) across three repeated experiments. Experimental conditions were the optimized conditions shown in the Experimental section.

reported electrochemical method,[28] and lower than the commonly used pNPP methods using *para*-nitrophenyl phosphate (pNPP) as a chromogenic substrate.[29,30] This demonstrated that the proposed method could be used for the detection of SAP with high sensitivity. Furthermore, the method also exhibited a good reproducibility for SAP detection. The RSDs of four repeated assays for 2 U mL^{-1} SAP and 0.4 U mL^{-1} SAP were 5.4% and 5.9%, respectively.

Fig. S8† shows the selectivity of the sensing platform for SAP detection compared to other interfering proteins. As shown in Fig. S8,† the addition of 0.2 μM BSA, IgG, PDGF-BB, SA yielded only negligible fluorescence changes when compared to that of SAP alone, indicating that the proposed strategy achieved high selectivity towards SAP and was able to detect SAP among other interfering proteins.

Assay of phosphatase in biological sample

To evaluate the practical utility of the proposed strategy, the label-free sensing platform was applied in a complex biological sample environment. In this assay, the sensing platform was applied to analyze DNA 3′-phosphatase in a diluted fetal bovine serum (FBS) sample. The reaction mixture was incubated with a high concentration of GO to avoid potential interference. Fig. S9† displays the bar graph of the corresponding fluorescence responses at 524 nm of the DNA 3′-phosphatase assay in diluted serum or buffer. As shown in Fig. S9,† there was no significant difference between the fluorescence intensities of the assay in buffer and in the diluted serum under the same concentration of DNA 3′-phosphatase. These results revealed that the proposed assay strategy was still highly specific to DNA 3′-phosphatase in a complex biological sample.

Effect of inhibitors on the dephosphorylation reaction

The established strategy can be further adapted to study the effects of inhibitor compounds on the phosphatase activities of T4 PNKP and SAP. Heparin and Na_3VO_4 have been reported to be inhibitors of T4 PNKP and alkaline phosphatase, respectively. Furthermore, the activity of KF polymerase was not affected by those two inhibitor compounds under the experimental conditions (data not shown). Fig. 5A shows the effect of heparin on the activity of T4 PNKP. As the heparin concentration increased, the relative activity of T4 PNKP decreased sharply. The half-maximal inhibitory concentration (IC50) of heparin was acquired from the plot of relative activity of T4 PNKP *versus* heparin concentration and was found to be 0.16 μg mL^{-1}. Fig. 5B shows the effect of Na_3VO_4 on the activity of SAP. As shown in Fig. 5B, the relative activity of SAP sharply reduced as the concentration of Na_3VO_4 increased.

The IC50 value of Na_3VO_4 was found to be 7 μM. As demonstrated by the above experimental results, the proposed method could be readily applied to assay two different DNA 3′-phosphatases, and the inhibition effect of the inhibitor compounds on the phosphatase activities of T4 PNKP and SAP could also be quantitatively evaluated.

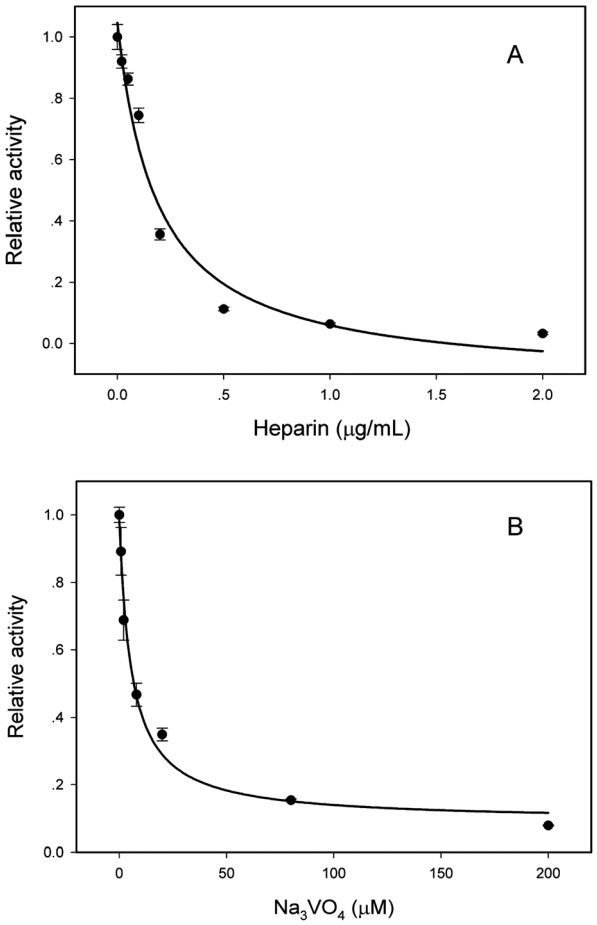

Fig. 5 (A) Influence of heparin on the relative activity of T4 PNKP. The concentration of T4 PNKP is 100 U mL^{-1}. The concentrations of heparin are 0, 0.02, 0.05, 0.1, 0.2, 0.5, 1.0 and 2.0 μg mL^{-1}, respectively. (B) Influence of heparin on the relative activity of SAP. The concentration of SAP is 2 U mL^{-1}, while the concentrations of Na_3VO_4 are 0, 0.8, 2, 8, 20, 80 and 200 μM, respectively. Experimental conditions were the optimized conditions shown in the Experimental section. The relative activity is defined as $(F - F_{blank})/(F_0 - F_{blank})$. F_0 stands for the fluorescence intensity from 100 U mL^{-1} T4 PNKP or 2 U mL^{-1} SAP; F is the fluorescence intensity from the varying concentration of inhibitors at the concentration of DNA 3′-phosphatases. F_{blank} is the fluorescence intensity without addition of T4 PNKP or SAP.

Conclusions

In conclusion, a novel and label free GO-based sensing platform for the assay of DNA 3′-phosphatases and their inhibitors was developed based on a hairpin primer and polymerase elongation. The assay relies on the principle that the polymerase elongation reaction is only initiated at the 3′-hydroxyl end of the primer, and double-strand selective staining of the elongation product. The proposed strategy is simple and convenient, yet still showed high sensitivity and selectivity, due to the introduction of GO as an efficient signal-to-background enhancer combined with SG-assisted fluorescence amplification. Our method was also used to investigate the effects of inhibitor compounds on the phosphatase activities of DNA 3′-phosphatases and satisfactory results were obtained. In addition, the proposed strategy was applicable to a real biological sample.

Given the simplicity, selectivity and sensitivity of this method, the proposed strategy may become a method of choice for the assay of DNA 3′-phosphatases and will find application in the study of DNA damage repair mechanisms.

Acknowledgements

This work was supported by NSFC (21025521, 21035001, 21190041), National Key Basic Research Program (2011CB911000), CSIRT Program and NSF of Hunan Province (10JJ7002).

Notes and references

1 R. A. Deshpande and T. E. Wilson, *Biochemistry*, 2004, **43**, 8579–8589.
2 Y. J. Song, K. G. Qu, C. Zhao, J. S. Ren and X. G. Qu, *Adv. Mater.*, 2010, **22**, 2206–2210.
3 W. D. Henner, S. M. Grunberg and W. A. Haseltine, *J. Biol. Chem.*, 1983, **258**, 15198–15205.
4 S. W. Yang, A. B. Burgin Jr, B. N. Huizenga, C. A. Robertson, K. C. Yao and H. A. Nash, *Proc. Natl. Acad. Sci. U. S. A.*, 1996, **93**, 11534–11539.
5 A. Jilani, D. Ramotar, C. Slack, C. Ong, X. M. Yang, S. W. Scherer and D. D. Lasko, *J. Biol. Chem.*, 1999, **274**, 24176–24186.
6 V. Cameron and O. C. Uhlenbeck, *Biochemistry*, 1977, **16**, 5120–5126.
7 M. Fanta, H. Zhang, N. Bernstein, M. Glover, F. Karimi-Busheri and M. Weinfeld, *Hybridoma*, 2001, **20**, 237–242.
8 L. K. Wang and S. Shuman, *J. Biol. Chem.*, 2001, **276**, 26868–26874.
9 C. Song, C. Zhang and M. P. Zhao, *Chem.–Asian J.*, 2010, **5**, 1146–1151.
10 C. Zhang, X. Su, Y. Liang, X. C. Zhu, C. Song and M. P. Zhao, *Biosens. Bioelectron.*, 2011, **28**, 13–16.
11 K. W. Lee, K. Maisel, J. M. Rouillard, E. Gulari and J. S. Kim, *Chem. Mater.*, 2008, **20**, 2848–2850.
12 K. J. Feng, L. P. Qiu, Y. F. Yang, Z. S. Wu, G. L. Shen and R. Q. Yu, *Biosens. Bioelectron.*, 2011, **29**, 66–75.
13 X. Zhu, X. M. Zhou and D. Xing, *Biosens. Bioelectron.*, 2011, **26**, 2666–2669.
14 X. L. Li, X. R. Wang, L. Zhang, S. W. Lee and H. J. Dai, *Science*, 2008, **319**, 1229–1232.
15 Y. J. Song, K. G. Qu, C. Zhao, J. S. Ren and X. G. Qu, *Adv. Mater.*, 2010, **22**, 2206–2210.
16 S. Stankovich, D. A. Dikin, G. H. B. Dommett, K. M. Kohlhaas, E. J. Zimney, E. A. Stach, R. D. Piner, S. T. Nguyen and R. S. Ruoff, *Nature*, 2006, **442**, 282–286.
17 C. H. Lu, H. H. Yang, C. L. Zhu, X. Chen and G. N. Chen, *Angew. Chem., Int. Ed.*, 2009, **48**, 4785–4787.
18 S. J. He, B. Song, D. Li, C. F. Zhu, W. P. Qi, Y. Q. Wen, L. H. Wang, S. P. Song, H. P. Fang and C. H. Fan, *Adv. Funct. Mater.*, 2010, **20**, 453–459.
19 H. X. Chang, L. H. Tang, Y. Wang, J. H. Jiang and J. H. Li, *Anal. Chem.*, 2010, **82**, 2341–2346.
20 H. Jang, Y. K. Kim, H. M. Kwon, W. S. Yeo, D. E. Kim and D. H. Min, *Angew. Chem., Int. Ed.*, 2010, **49**, 5703–5707.
21 X. H. Zhao, R. M. Kong, X. B. Zhang, H. M. Meng, W. N. Liu, W. H. Tan, G. L. Shen and R. Q. Yu, *Anal. Chem.*, 2011, **83**, 5062–5066.
22 Y. Wang, Z. H. Li, D. H. Hu, C. T. Lin, J. H. Li and Y. H. Lin, *J. Am. Chem. Soc.*, 2010, **132**, 9274–9276.
23 C. H. Lu, J. Li, M. H. Lin, Y. W. Wang, H. H. Yang, X. Chen and G. N. Chen, *Angew. Chem., Int. Ed.*, 2010, **49**, 8454–8457.
24 C. H. Lu, C. L. Zhu, J. Li, J. J. Liu, X. Chen and H. H. Yang, *Chem. Commun.*, 2010, **46**, 3116–3118.
25 Y. Zhang, Y. Liu, S. J. Zhen and C. Z. Huang, *Chem. Commun.*, 2011, **47**, 11718–11720.
26 Y. G. Li and Y. Y. Wu, *J. Am. Chem. Soc.*, 2009, **131**, 5851–5857.
27 L. Lin, Y. Liu, X. Zhao and J. H. Li, *Anal. Chem.*, 2011, **83**, 8396–8402.
28 P. Miao, L. M. Ning, X. X. Li, Y. Q. Shu and G. X. Li, *Biosens. Bioelectron.*, 2011, **27**, 178–182.
29 A. E. Marley, J. E. Sullivan, D. Carling, W. M. Abbott, G. J. Smith, I. W. Taylor, F. Carey and R. K. Beri, *Biochem. J.*, 1996, **320**, 801–806.
30 R. Xiao, L. Xie, J. Lin, C. Li, Q. Chen, H. Zhou and R. Zhang, *J. Mol. Catal. B: Enzym.*, 2002, **17**, 65–74.